



REAL STRUCTURE DEPTH PROFILE OF SHOT-PEENED SURFACE OF A CORROSION-RESISTANT STEEL

J. Drahokoupil^{1,2}, N. Ganev¹, M. Čerňanský², M. Stranyánek^{2,3}, R. Čtvrtlík^{2,3}

¹Faculty of Nuclear Sciences and Physical Engineering, Czech Technical University, Trojanova 13, 120 00 Praha 2, Czech Republic.

²Institute of Physics of the ASCR, v.v.i., Na Slovance 2, 182 21 Praha 8, Czech Republic

³Joint Laboratory of Optics of Palacky University and Institute of Physics of the ASCR, v.v.i., 17. listopadu 50, 772 07 Olomouc, Czech Republic.
jandrahokoupil@seznam.cz

Keywords:

X-ray diffraction, steels, gradients, real structure

Abstract

The main goal of this paper is to characterize surface layers of corrosion-resistant steel affected by shot peening. Several experimental methods were used for investigation of samples prepared by using two different levels of shot peening intensity. X-ray diffraction was applied as a main technique for crystallite size, microscopic and macroscopic residual stress determination. Combination of X-ray diffraction with electrolytic polishing enables to study the depth profile of aforesaid quantities. Nanoindentation and optical microscopy were also applied on polished cross sections of the samples. It was observed that more intensively shot-peened sample differs from the sample blasted with lower particle's intensity mainly in the width of affected zone, which was ca. 0.4 mm and ca. 0.2 mm respectively. Significant correlation was observed between the depth profiles of macroscopic residual stress and crystallite size. No change in phase content due to surface treating was found.

Introduction

X-ray residual stress measurement ranks among those applications of X-ray diffraction that are very useful in metals, alloys and ceramics industrial treatment processes [1]. It is evident that if residual stresses can be specified (measured), it will be possible not only to prevent their harmful effects, but also to utilize their beneficial impact. Shot peening is a cold working process in which the surface of a part is bombarded with small spherical particles (shots). Benefits obtained by shot peening are the result of the magnitude and depth distribution of the compressive residual stresses and the cold working induced [2].

The aim of the contribution is to present a complete X-ray diffraction analysis of gradients of crystallite size and of both the macroscopic and microscopic residual stresses in surface layers of shot-peened samples. Two different conditions of blasting were applied to samples under investigation. The main goal of the research is to find correlations between lattice deformation of the studied sur-

faces and their mechanical properties, and this way to contribute to understanding of the onset of residual stress formation in engineering materials.

Samples

The samples of size 50 × 50 × 5 mm³ were prepared from corrosion-resistant steel ČSN 17134. The guaranteed corrosion resistance on air, water steam or gas is up to 625 °C. The material is used for some parts of turbine or for thick-walled steam supply pipe. The chemical composition is in Tab. 1. Prior to shot peening the samples were annealed (stress-relieved) in *Ar* at 550 °C for 2 hours.

The shot peening was carried out with two different intensities of blasting specified by using *Almen test* as 0.2 mmA (sample C11) and 0.4 mmA (sample C13) [3].

Polished cross sections (10 × 5 mm²) prepared from the samples were used for nanoindentation experiments and for microscopic observations.

Methods

X-ray diffraction

The measurement was performed on an θ -goniometer Siemens with Cr-K radiation. The line {211} of γ -Fe phase was measured. Nine different tilts angles (θ) from 0° to 63° were used. The \sin^2 method was used for determination of macroscopic residual stresses [4]. The X-ray elastic constants $1/2s_2 = 5.95 \cdot 10^{-6} \text{ MPa}^{-1}$, $-s_7 = 1.325 \cdot 10^{-6} \text{ MPa}^{-1}$ were used in stress calculations. The single line Voigt function method was applied for corrections of instrumental broadening (standard was measured for all nine inclination) and determination of microstrains and crystallite size [5]. The microstrains ϵ was converted to microstresses ϵ^{micro} using Hooke's law ($\epsilon = e E$, where the Young modulus $E = 216 \text{ GPa}$) in order to have the possibility of their comparison to the macroscopic residual stress ϵ^{macro} .

This procedure has some advantages and disadvantages as well. The main advantage is that the macroscopic and microscopic strains are determined from the same crystallographic planes. Then the data are unaffected by elastic anisotropy, which is relatively large in iron. The another advantage is the high diffraction angle θ of the {211} γ -Fe line ($2\theta = 156^\circ$) enabling a precise determination of lattice

Table 1. The chemical composition of investigated steel 17 134 in weight percent.

C	Mn	Si	Cr	Ni	Mo	V	P	S
0.17-0.23	0.50-1.00	0.25-0.60	10.0-12.5	0.30-0.80	0.80-1.20	0.20-0.35	max 0.035	max 0.030

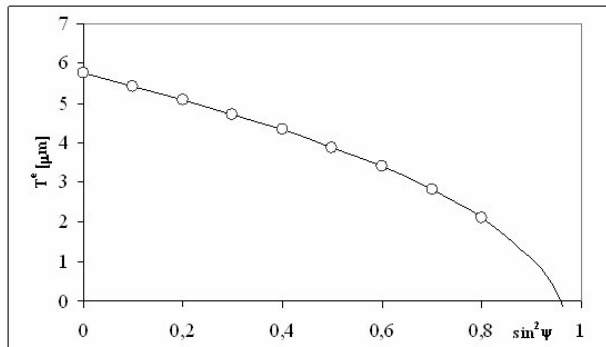


Figure 1. The dependence of effective penetration depth T^f on \sin^2 in case diffraction angle $\theta = 156^\circ$, Cr – radiation, and Fe matter.

strains. A disadvantage is that a separation of broadening diffraction line to crystallite size and microstrain contributions using any single line methods is not as precise as when several lines are considered. Realizing that the penetration depth for each of the three diffraction lines ($\{110\}$, $\{200\}$, $\{211\}$) of α -Fe when Cr-K radiation is used, is different application of methods using several diffraction lines is problematic. Since the intensity of radiation is exponentially decreased in the matter, the effective penetrations depth T^f is used to describe radiation penetrate ability [6]. Fig. 1 describes the effective penetration depth vs. \sin^2 in case the Cr – radiation (wavelength $\lambda = 0.228962$ nm) in Fe (density $\rho = 7.874$ g/cm³) for the diffraction angle $\theta = 156^\circ$.

In order to obtain depth profiles of X-ray diffraction characteristics, the surface layers were removed by a *LectroPol-5* device for electrolytic polishing. The cooling system maintains the temperature in the range of 15 – 25 °C. The sample C11 after removal of 0.8 mm is in Fig. 2.

Nanoindentation

The used apparatus *NanoTestTM NT600* enables DSI (depth sensing indentation) experiments. These were performed with a diamond Berkovich indenter. Calculations of indentation hardness and effective elastic modulus E_r were made according to Oliver-Pharr method [7] from DSI

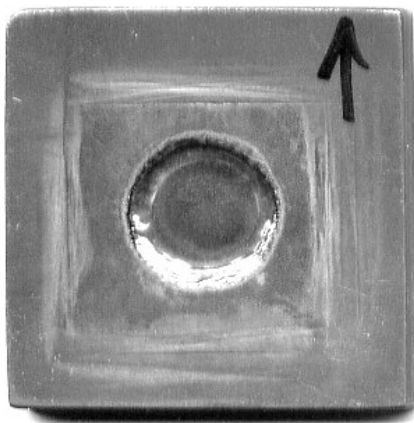


Fig. 2. The sample C11 after multiple removing of surface layers.

unloading curves. Each sample was indented in five different points on polished cross section at increased distance from treated surface (matrix 5 x 14). Maximal load was 50 mN; loading/unloading time was 20 s; dwell time at maximal load was 10 s.

Microscopy.

Zeiss Axio Imager Z1m optical microscope was used to study cross section of the samples.

Results and discussions

X-ray diffraction

The samples were measured in two each to another perpendicular directions labelled as “ \rightarrow ” and “ \uparrow ” in order to verify the directional independences of the residual stresses. The single line Voigt function method [5] gives values of crystallite size D and microstrain e (or ϵ^{micro}) for every tilt angle ψ , i.e. for $\sin^2 = 0, 0.1, 0.2, \dots 0.8$. The individual values depend on gradients, orientation of diffracting planes (angle θ), and inaccuracy of used procedures. Fig. 3 and 4 show the dependences of crystallite size D and microstresses σ on orientation of diffraction planes to the surface. The obtained values for both directions are plotted for surface values and for values from the depth of 0.8 mm. The dependence of studied parameters on angle ψ is caused by gradients, by θ -orientation dependence, and by some inaccuracies originated in a processing of measured data (e.g., profile fitting by analytical Pearson VII function, gradients, using of convolution instead of solving integral equations, ...).

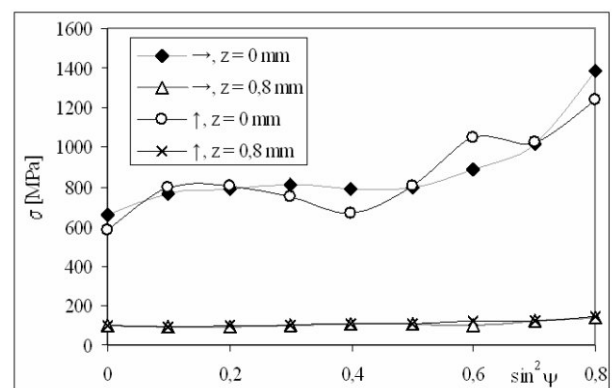


Figure 3. The dependence of microstresses on \sin^2 .

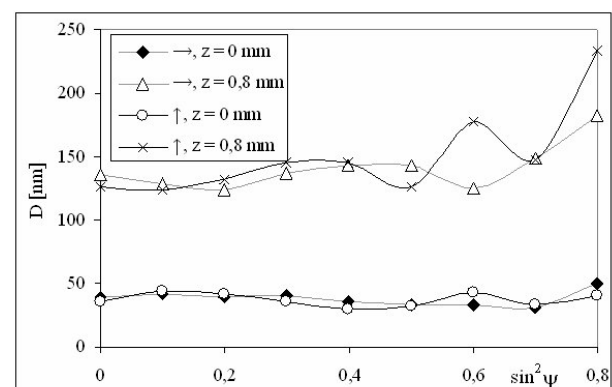


Figure 4. The dependence of crystallite sizes on \sin^2 .



Table 2. The depth profile of D , σ^{micro} and σ^{macro} for sample C11. The signs \uparrow and \rightarrow marked two perpendicular directions.

z [μm]	D		σ^{micro}		σ^{macro}	
	\uparrow	\rightarrow	\uparrow	\rightarrow	\uparrow	\rightarrow
0	37	37	879	856	-579	-580
25	48	52	571	629	-569	-584
40	55	50	522	506	-589	-588
60	57	53	384	368	-584	-587
80	55	53	315	313	-576	-565
110	60	66	210	194	-513	-489
150	116	121	169	159	-245	-181
200	138	141	122	128	-45	-47
250	115	114	107	113	-27	-27
360	138	130	110	108	1	-5
470	133	128	111	112	7	4
600	129	132	103	103	28	31
800	139	145	107	110	16	19

Table 3. The depth profile of D , σ^{micro} and σ^{macro} for sample C13. The signs \uparrow and \rightarrow marked two perpendicular directions.

z [μm]	D		σ^{micro}		σ^{macro}	
	\uparrow	\rightarrow	\uparrow	\rightarrow	\uparrow	\rightarrow
0	26	33	842	1090	-519	-552
25	47	44	844	819	-570	-580
40	47	47	721	718	-596	-607
60	48	52	563	610	-601	-622
80	53	54	468	472	-610	-627
110	53	55	382	409	-595	-601
150	55	57	227	236	-540	-570
200	72	70	188	181	-493	-514
250	90	91	167	165	-352	-338
360	131	142	108	112	-4	17
470	135	151	108	114	10	-23
600	128	131	110	108	10	12
800	133	136	107	106	29	18

In order to compare these data with macroscopic residual stress, the values for all tilts were averaged. Tab. 2 and 3 show the values of crystallite size D , microstress σ^{micro} and macrostress σ^{macro} determined for samples C11 and C13.

For reasons of clarity the average values for these perpendicular directions are plotted in Fig. 5. Predication that shot peening is symmetrical treatment [3], give us the competence for the mentioned averaging. The depth profiles of crystallite size are plotted in Fig. 6 for both orientations. The absolute value of crystallite size and microstress are encumbered by relatively large errors, caused primarily by following reasons: (i) The problem in determination of z (the radiation is exponentially decreased in the material), (ii) Strong presumptions of single line Voigt function method [5], (iii). Inaccuracy of used Young modulus (tabu-

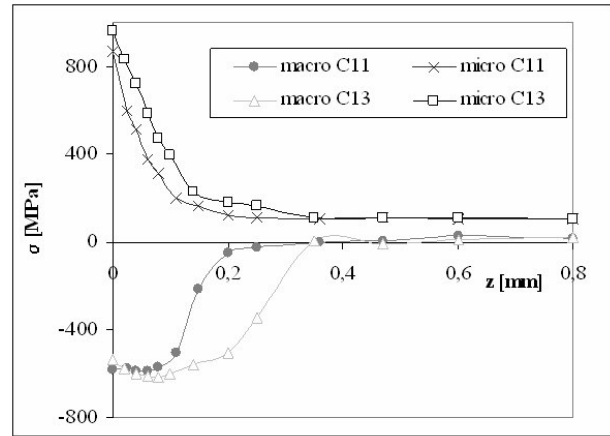


Figure 5. The depth profile of micro and macro stresses for two intensity of shot-peening – C11 and C13.

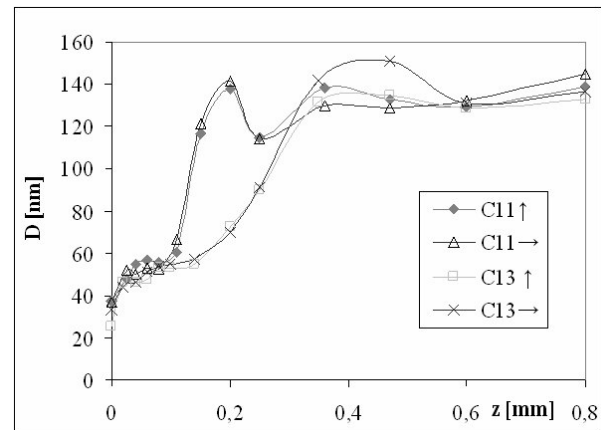


Figure 6. The depth profile of crystallite size D for two directions \uparrow and \rightarrow and for two intensity of shot peening – C11 and C13.

Table 4. The correlation coefficients between particle size and macrostress ($D - \sigma^{macro}$), particle size and microstress ($D - \sigma^{micro}$),

	$D - \sigma^{macro}$	$D - \sigma^{micro}$	$\sigma^{micro} - \sigma^{macro}$
C11 \uparrow	0,97	-0,84	-0,79
C11 \rightarrow	0,98	-0,83	-0,80
C13 \uparrow	0,96	-0,83	-0,71
C13 \rightarrow	0,97	-0,79	-0,68

lated values from single crystal was used), that was used in computing of stresses. This problems are not so significant when relative values are ratiocinate. The values for two different directions can provide the view to errors of their determination.

Table 5. The average results of nanoindentation experiments for both samples.

	Max. depth [nm]	Contact Depth [nm]	Max. load [mN]	Hardness [GPa]	Er [GPa]	Plastic work [nJ]	Elastic work [nJ]
C11	748	702	50	4,0	205	11,9	1,9
C13	746	700	50	4,0	204	11,9	1,9

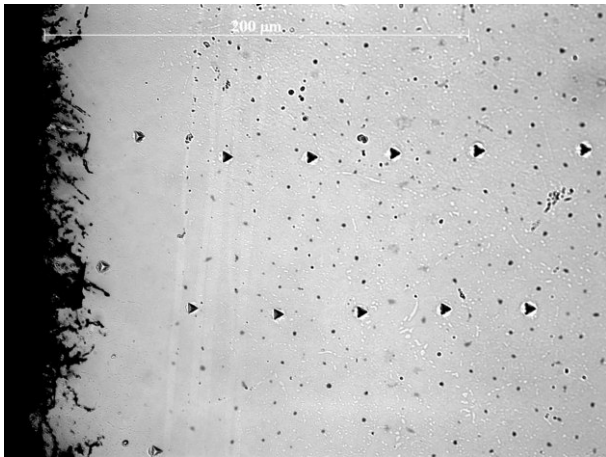


Figure 7. Sample C11, zoom 50x.

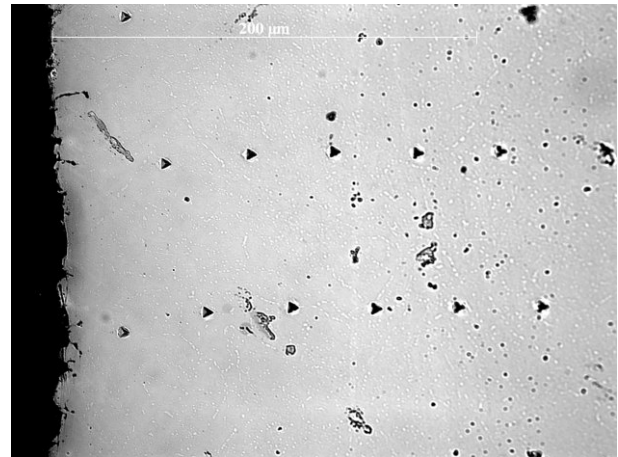


Figure 8. Sample C13, zoom 50x.

The thickness of the affected surface layers by shot peening is roughly 0.2 mm for sample C11, and 0.4 for sample C13 for all three quantities - D , D_{micro} and D_{macro} .

The values of correlations coefficient [8] calculated from Tabs. 2 and 3 are in Tab. 4.

The correlation coefficient has the value between -1 and $+1$, so two independent quantity have the correlation coefficient $r = 0$. The largest correlation was observed between crystallite size and macroscopic stress ($r = 0.97$). On the other hand, the smallest correlations are observed between macroscopic and microscopic stress ($r = -0.75$). The correlation is not as great as in the previous case, although a relation is present.

Nanoindentation

The nanoindentation experiment for samples C11 and C13 do not afford any larger increase or decrease of observable parameters of depth profile studies. So, only the average values of observed parameters are putted in Tab. 5.

Microscopy

The samples were observed in an optical microscope after nanoindentation experiments (Figs. 7. and 8). The treated surfaces are on the left side.

The sample C11 has the surface layer largely disturbed. The black triangles are residual nanoindentation impressions. The small black points are probably small pores; they come to be sharp the same way as triangles after nanoindentations. Moreover, the X-ray diffraction phase analysis did not show difference between treated sample and not-treated one. Fig. 9 displays the diffraction pattern

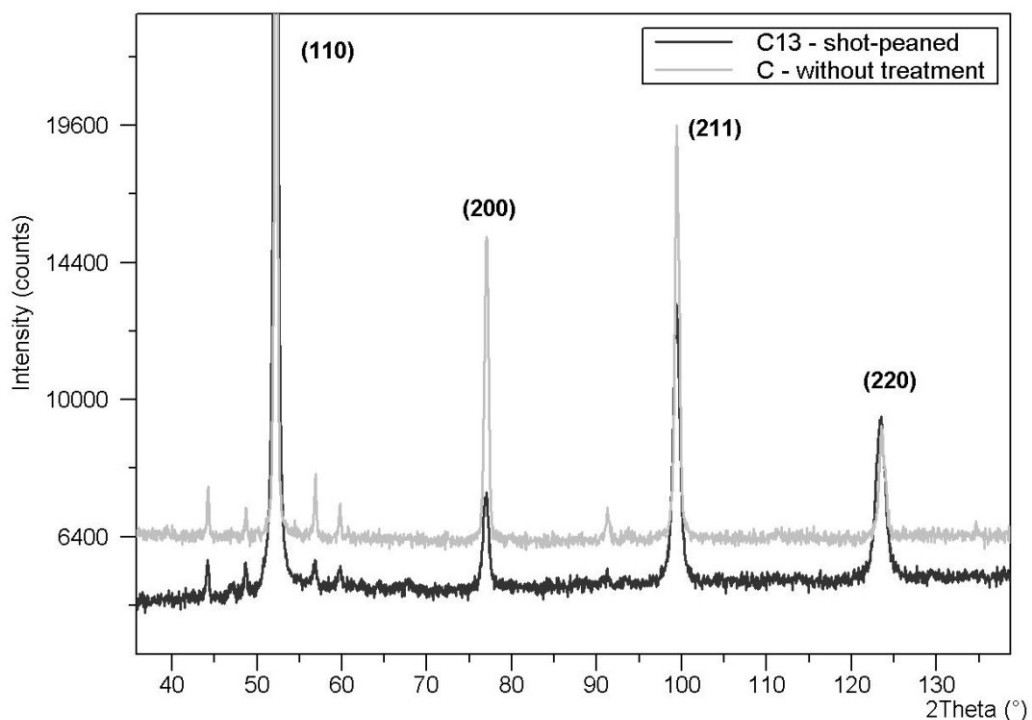


Figure 9. Main part of x-ray diffraction patterns for treated and non-treated sample. The shot-peened pattern is putted down by 1000 counts for better visibility. The main four peaks, labeled with their respective diffraction planes, corresponds to Fe- phase.



of these two cases measured with Co-K α radiation. The more intensive peaks are from γ -Fe phase. The small peaks are from nonspecific phases. Their low intensities and insufficient number do not allow the regular phase analysis. Nevertheless matching these peaks with PDF database [9] lead to the result that there is more than one probable phase and the most possible phases are: Fe₃C, Fe₂C, C, Cr₂₃C₆, Cr_{21.34}Fe_{1.66}C₆ (and phases with similar composition), MnC.

Conclusions

In the case of the studied steel ČSN 17 134 X-ray diffraction measurements afford a more precise idea about surface layers affected by shot peening than nanoindentation and microscopy. Nevertheless comparison of results obtained by these three methods provides different points of view to characterisation of treated surface.

- More intensively shot-peened sample has wider affected layer than the one shot-peened with lower intensity. While the width in the first case is ca. 0.4 mm, the corresponding value the second one being ca. 0.2 mm.
- The surface values of crystallite size and macrostress are approximately the same for both the intensities of blasting. The differences are observed primarily in the specific interval of depth, which is in good accordance with the observation in optical microscopy.
- Aside to the crystallite size and macrostress, the surface values of microstress of differently shot-peened samples are different and the microstress increases with the intensity of shot peening.
- The values of macrostress significantly correlate with those of crystallite size; the correlation coefficient is approx. 0.97.

The micrographs obtained from the optical microscope suggests that the shot peening has an influence on the phase

composition. However, the results of X-ray phase analysis did not affirm this and black points in Figs. 7, 8 are interpreted as small pores.

Acknowledgement

The research was supported by the Project No. 106/07/0805 of the Czech Science Foundation.

References

1. V. Hauk (ed.), Structural and Residual Stress Analysis by Nondestructive Methods, Elsevier Science B. V., 1997, 640 p.
2. I. Kraus, N. Ganey, in *Industrial Applications of X-Ray Diffraction*, New York, Marcel Dekker 1999.
3. N. Ganey, M. Čerňanský, J. Drahokoupil, K. Kolařík. CD-ROM of Proceedings EAN 2005, June 7-9, 2005, Skalský Dvůr, Czech Republic.
4. U. Welzel, J. Ligot, P. Lamparter, A. C. Vermeulen and E. J. Mittemeijer, *J. Appl. Cryst.*, **3**, (2005), 1.
5. Th.H. de Keijser, J.I. Langford, E.J. Mittemeijer, A.B.P. Vogels, *J. Appl. Cryst.*, **15**, (1982), 308.
6. J. Drahokoupil, M. Čerňanský, N. Ganey, K. Kolařík, Z. Pala, *Solid State Phenomena*, **130** (2007) pp. 77-80.
7. W. C. Oliver, G. M. Pharr, *J. Mater. Res.*, **7**, (1992) 1564.
8. Brandt, S.: *Statistical and Computational Methods in Data Analysis*. North Holland Publishing, New York, 1970.
9. PDF – Powder Diffraction File. The International Centre for diffraction Data (<http://www.icdd.com>).